A Photo Voltaic System Based Dual Inverter

[1] S.Sarada, [2]C.Ganesh [3] L.Chandra kanth
Department of Electrical Engineering,
Annamacharya Institute of Technology and Sciences, Rajampet-516126

Abstract: -- This scheme presents an integrated solution for Photo Voltaic cell(PV) fed water-pump drive machine which uses an Open-End Winding Induction Motor (OEWIM). The dual inverter fed OEWIM drive achieves the functionality of a three level inverter and needs low value DC bus voltage. This helps in optimal arrangement of Photo voltaic cells, this can avoid large strings and helps in improving the PV performance with wide band-width of operating voltage. It also reduces the voltage rating of the DC-link capacitors and switching devices used in the system. The proposed control scheme achieves an integration of both Maximum Power Point Tracking (MPPT) and *V/f* control for the efficient utilization of the PV panels and the motor. The proposed control scheme requires the sensing of PV voltage and current only. Thus, the system requires less number of sensors.

Index Terms—Photo voltaic cell, centrifugal pump, maximum power point tracking, open-end winding induction motor

I. INTRODUCTION

More than 40% of total electric power is consumed by the electrical motors. Modernization of human society and growing application of electric motors, have exponentially increasing the demand for electrical energy. This leads to increase in the power generation capacity. However, due to ecological concerns, restriction and constraints are imposed on increasing the generation capacity of conventional sources. So contemporary research is focused towards an effective utilization of non-conventional sources. Among the different available non-conventional sources Photo Voltaic (PV) technology seems to be the most attractive and promising . This can be attributed to decrease cost of PV modules, free energy source, zero maintenance, and noise free operation. Thus, purpose of PV source for powering electric motor could be a good solution especially for water-pumps, electric fans, submersible pumps etc. Such loads can have the option of optimally using PV power whenever Sun power is available. Further, when such loads are used in the stand-alone system like water pumping application in agricultural, industrial and domestic sectors, solar PV powered system could be a better solution. It could meet the requirement during danger situation i.e., during summer particularly in tropical countries like India. This utilizes the use of electric motor-pump with good performance and better efficiency with the PV system. Some possible solutions given for PV fed water-pump were based on usage of DC motor either via a DC-DC or directly coupled converter with PV source. However, the requirement of continuous maintenance and higher cost restricts the use of DC motors for their application in PV water pumping systems. Thus, there is a need of such a

solution that uses the PV power effectively, while using a low cost, low maintenance, reliable and robust motor for pumping application. The most suitable motor for such application is an Induction Motor (IM). Some of the first proposals for a Photo voltaic fed IM, based on two-stage system were given by various authors in the past.
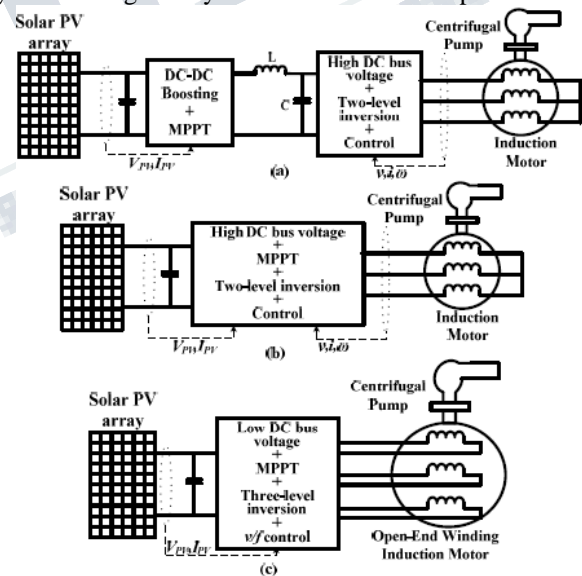
Fig.1.Block diagram of PV powered centrifugal pump (a) Conventional two-stage; (b) Conventional single-stage; (c) Proposed single-stage.

Most of them have used a DC-DC boost converter in the first stage and the second-stage comprises of a DC-AC inverter. Boost converter amplifies and operates the low value PV input voltage near Maximum Power Point (MPP)

while the inverter gives the required AC voltage to the IM. Also, the control techniques are based on either independent frequency control, or a *V/f* control. Recently, a proposal based on closed loop speed control to improve the performance and efficiency of the system was given by Montiê Alves Vitorino*et. al*., in which the authors have presented a sensor-less speed control technique. However, two-stage power conversion, high voltage rating of semi-conductor devices and more number of sensors increase the power loss and cost of the system.

A typical PV pumping system with two power conditioning stage is shown in Fig. 1(a). As discussed earlier, this system results in poor performance and lesser efficiency. Therefore, a single-stage system with simpler control as shown in Fig. 1(b), could be a better choice . One of such a system was proposed by Eduard Muljadi , in which the author have used a six-step quasi square wave inverter, which can take care of DC-AC inversion as well as Maximum Power Point Tracking (MPPT) for the PV source. It is a better proposition since the author has given an integrated single-stage power conversion solution. But the drawback of this system is that, the six-step quasi-square inverter deteriorates the motor performance and hence the efficiency. It also requires filters, which are bulky and expensive. Further, this system requires a higher voltage rating for the input DC-link capacitor and semiconductor devices. All these may increase the cost, weight, size and power loss of the system.

Recently, Messaoud Makhlouf*et. al.* have suggested the closed loop vector control for PV pumping system using a single-stage multi-level Pulse Width Modulation (PWM) converter. While this system results in low motor losses, it is more complex with more number of control variables and sensors. Most recently, Tomás Perpétuo Corrêa*et. al.* have published a paper with a stand-alone PV pumping system. It is also a single-stage system, wherein the authors have proposed MPPT and Minimum Losses Point Tracking (MLPT) methods of control. However, this system requires more number of sensors, and results in low band-width for PV operating voltage.
Thus, from the above discussion, it is evident there is a requirement for a low-cost, low-voltage single-stage power conversion PV water pumping system with wide bandwidth of PV operating voltage. Also, the three-level/multi-level inverter with a low DC bus voltage could be a better solution as the performance of this system improves with

the increased number of levels/steps in the inverter output voltage. Also, many investigations on Open-End Winding Induction Motor (OEWIM) with multilevel inverters are documented in the literature . Further various PWM techniques and control schemes for OEWIM drive have been analyzed by various researchers. In short, OEWIM promises to provide effective solutions for drive application as compared to common neutral IM . Apart from high reliability and redundancy OEWIM has many good features as discussed in the next paragraph.

One of the most important feature of OEWIM is it uses two two-level Voltage Source Inverters (VSIs) to achieve three level inversion. It also lowers voltage rating of semiconductor devices and input DC bus electrolytic capacitor . This can be attributed to the fact that DC bus voltage is designed based on maximum value of phase voltage instead of line to line voltage. The decoupled PWM technique increases the apparent switching frequency of switching devices, reducing the ripple in the motor phase current. Unlike the conventional three-phase Neutral Point Clamped (NPC) three level inverter, wherein the DC-link capacitor is constrained to carry load current leading to large fluctuations of voltage of the DC-neutral point, the DC-link capacitor of OEWIM carries only the ripple current, thus resulting a negligible voltage fluctuations . This increases the life and reliability of the DC bus capacitor or in other words the reliability of the inverter system, which is of paramount interest for systems connected to PV source.
Thus, OEWIM coupled with PV source could be a good proposition. This paper presents one such solution for a simple water-pump application as depicted in Fig. 1(c). The proposed system has the following features:

1. It is an economical system as it uses a single power conditioning stage.

2.It has inherent low DC bus voltage requirement with *V/f* control integrated with MPPT and uses three-level (DCAC)inversion for better performance of motor.

3.Low input DC bus voltage requirement reduces the voltage rating of DC-link capacitor and increases bandwidth of PV operating voltage. It also reduces the voltage rating of the semi-conductor devices used in the inverter.

4.It optimally uses PV source for all environmental conditions by operating at MPP. Also, it employs *V/f* control integrated in MPPT algorithm which improves the performance of the motor and requires less number of sensors for its operation.

5.Three-level output with Decoupled Sample-Averaged Zero sequence Elimination (DSAZE) algorithm further improves the performance with reduced motor current ripple.

Rest of the manuscript is divided into four sections. Second section gives details of modeling of the proposed system. Third section describes the operation and analysis of the proposed system. Fourth section describes the control strategy and algorithm proposed. Fifth section depicts the simulation and experimental results obtained. It also gives the detailed cost analysis and comparison for the proposed system with the existing system(s).

II. MODELING OF THE PROPOSED SYSTEM

A proposed configuration of the solar PV powered pumping system is shown in Fig. 2, which comprises of 1) solar PV array; 2) dual-inverter namely inverter-I and inverter-II; 3) three-phase open-end winding induction motor with pump load; 4) controller block which consists of MPPT and DSAZE PWM algorithm. These components are described in detail in the following sub-sections.

A. PV source Model

The PV source was modeled by using PV cell *current voltage* characteristic equation as furnished below
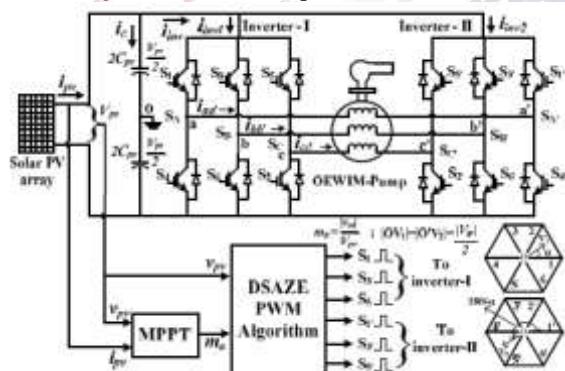
Fig .2.Schematic circuit diagram of proposed system

$ipvcell = iL - io(e\ q(vpvcell+ipvcell\ Ra\ )/nKT\ -l)$ (1)

where *ipvcell*: PV cell current; *iL*: photo-current; *i0* : Diode saturation current; *n* : Diode quality or ideality factor; *k* : Boltzmann constant; *q*: electron charge; *T* : panel operating temperature in Kelvin; *Rs*: PV cell series resistance; *Vpvcell*: PV cell voltage (V).

The output of PV source is connected to inverter with DC bus capacitance *Cpv*. By applying KCL at input of inverter (from Fig. 2)

$ipv=ic+iinv ==Ipv= Cpvdvpv/dt +ipv$ (2)

Integral solution of (2) is the voltage vpv across capacitance Cpv, which is used by the PV model to calculate the PV source current. The inverter current iinv is the current drawn by inverters I and II. Further dual-inverter has two series connected equal value capacitors across the DC-link. These capacitors share equal voltage with respect to the common point 'o' as shown in Fig. 2.

B. Modular three-level dual-inverter model:

Dual-inverter used in the proposed configuration is modeled using switching functions [30]. To model dual inverter, switching function *SW* (where *W* can be *A, B, C, A', B'or C'* depending on the phase and number of inverter) requires the logic generated from PWM controller. It has value 1 and -1 which represents turn ON of top and bottom switch respectively for the given leg or phase of the inverter. The modular dual-inverter shown in Fig. 2 consists of six poles (*a, b, c, a', b',* and *c'*) and twelve switches (two switches per pole). The value of the pole voltages in a particular phase can be ±*Vpv/2* depending on the switch (whether top or bottom) is turned ON. If top switch of phase 'a', *S1* is turned ON, the pole voltage vao is +*Vpv/2* and when bottom switch of phase 'a', *S4* is turned ON then the pole voltage vao is –*Vpv/2*. Thus, pole voltage of inverter-I can be given as

$Vao= SAVpv/2; Vbo=SB\ VPV/2;Vco=SCVpv/2$ (3)

Similarly, pole voltage of inverter-II can be given as

$Va'o= SA'\ Vpv/2; Vb'o=SB'\ VPV/2;Vc'o=SC'\ Vpv/2$ (4)

The motor phase voltage Vaa' is given by

$Vaa'= VPV/2[2/3(SA-SA') -1/3(SB-SB,)+(SC-SC')]$ (5)

Similarly the other phase voltages V*bb'*, V*cc'*of the inverter output can be derived for the system. Further the input inverter current *iinv* can also be derived using switching functions.

Current flowing through inverter-I is given by

iinv1= ½ (SA+1)iaa'+ ½ (SB+1) ibb'+ ½ (SC+1)icc'(6)

iinv2= ½ (SA,+1)(-iaa')+ ½ (SB,+1)(-ibb')+ ½ (SC,+1)(-icc') (7)

iinv= ½ (SA-SA')iaa' + ½ (SB-SB')ibb'+ ½ (SC-SC')icc' (8)

Thus the above values of phase voltage and current can be used by Simulink model of OEWIM, which is discussed in the next section.

C. Open-End Winding Induction Motor model

An Open-End Winding Induction Motor [28] is obtained by opening the neutral point of the star connected stator windings of a normal three-phase Induction motor. The winding diagram of three-phase OEWIM is shown in Fig. 3. For modeling and analysis the decoupled form of OEWIM is considered. For transforming the stator ($\phi=\theta$) and the rotor parameters ($\phi=\beta$) to decoupled form, the transformation matrix used is given in (9).

$$\begin{bmatrix} x_{qy} \\ x_{dy} \\ x_{0y} \end{bmatrix} = \frac{2}{3} \begin{bmatrix} \cos\phi & \cos(\phi - 2\pi/3) & \cos(\phi + 2\pi/3) \\ \sin\phi & \sin(\phi - 2\pi/3) & \sin(\phi + 2\pi/3) \\ 1/2 & 1/2 & 1/2 \end{bmatrix} \begin{bmatrix} x_{aa'} \\ x_{bb'} \\ x_{cc'} \end{bmatrix} \quad (9)$$

where, θ is the angle between the stator *as*-axis and the quadrature (q) axis, β is the angle between rotor *ar*-axis and the *q*-axis, also β=□-□r,□r is the angle between rotor *ar*-axis and stator *as*-axis (Fig. 3), parameter *x* can be either voltage '*v*' or current '*i*' or flux linkage 'λ' and subscript parameter *y* can be'*s*' or '*r*'. The subscript '*s*' denotes the parameters of stator and the subscript '*r*' denotes the parameters of rotor.The dynamic *d-q* model of an OEWIM is described by in(10) to (13).

vqs =Rsiqs +ω(LIsids +Lm(ids +i'ds)) +ρλqs (10)

vds =Rsids - ω(LIsiqs +Lm(iqs +i'qs)) +ρλds (11)

v'qs =R'ri'qs +(ω-ωr)(L'iri'dr +Lm(ids +I'ds)) +ρλ'qr (12)

v'dr =R'ri'dr–(ω-ω) (L'iri',qr +Lm(iqs +i'qr)) +ρλ'dr (13)

where, *Rr*– rotor resistance, *Rs*– stator resistance, *Lls*– stator leakage inductance, *L'lr*– rotor leakage inductance, *Lm* – mutual inductance between stator and rotor winding, *ω* is the synchronous speed, *ωr* is the electrical speed of motor, *p* denotes the time derivative. Also, here V'qr = V'dr =0, since rotor bars are short-circuited.

The expression for the electromagnetic torque *Tem* is given by

Tem =32*P*2 *L*m[iqsi'dr–idsi'qr] (14)
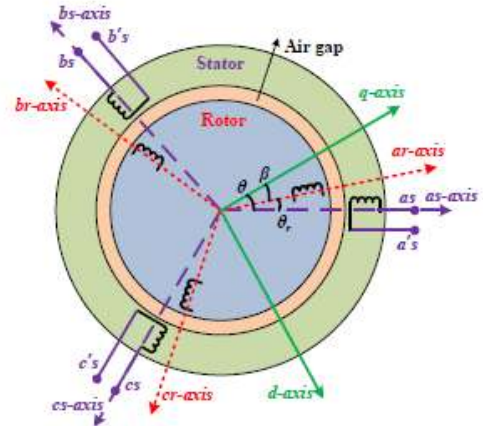
Fig. 3. Open-end winding induction motor model where, P is the number of poles.

The mechanical equation governing the OEWIM pump drive is expressed in (15) as

$$T_{em} = J\frac{d\omega_{rmech}}{dt} + B\omega^2_{rmech} + T_L$$

(15)

Where, *J* – motor inertia (kg-m2), *B* – centrifugal load torque coefficient, *TL* – load torque (N-m), ωrmech is instantaneous angular velocity of motor shaft (rad/sec).

III. OPERATION AND ANALYSIS OF THE PROPOSED SYSTEM

The proposed dual-inverter is operated by using the decoupled PWM strategy. It incorporates simple *V/f* control for the efficient operation of system below the rated speed.

The proposed PWM strategy requires the information of magnitude and angle of the reference voltage vector. The magnitude is calculated and controlled by the MPPT algorithm and the angle 'α' is the function of time and fundamental frequency of reference modulating waveform. The reference voltage vector $|vsr|\angle\alpha$ is further divided into two decoupled components $|vsr|/2\angle\alpha$ and $|vsr|/2\angle(180+\alpha)$. The decoupled components are then given as the reference vector for inverter-I and inverter-II respectively as shown in Fig. 2, for generation of required output voltage. Thus, using decoupled PWM configuration has the benefit of double output voltage.

Low input DC bus voltage requirement of dual-inverter for OEWIM-pump drive:

To analytically verify the low input DC bus voltage requirement, a comparison between two-level and dual inverter fed OEWIM is done. Both the inverters are compared for generating same output voltage vector with different values of input PV source voltage. The low input voltage requirement of dual-inverter for an OEWIM drive is demonstrated in Fig. 4.Let the PV source voltage required to generate the rated instantaneous induction motor phase voltage, *van* is *Vpv* as shown in Fig. 4(a). From Fig. 4(a) and 4(b) the inverter output voltage, Van, Vbn and Vcn can be obtained using the inverter pole voltage, Vao, Vbo and Vco; and switching functions *SA*, *SB* and *SC* as follows:
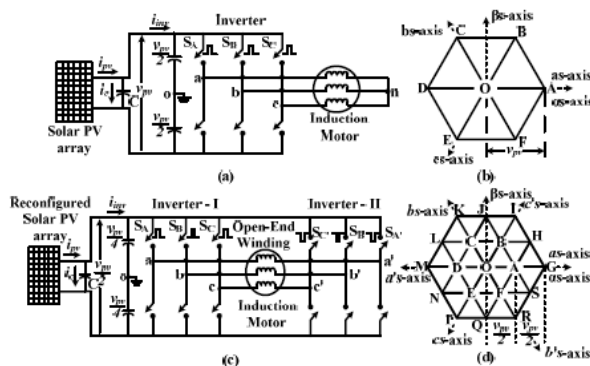
Fig. 4. Demonstration and comparison of DC bus voltage requirement for H bridge and dual-inverter systems. (a) Schematic circuit diagram of two-level H-bridge inverter with input DC voltage (PV voltage) of '*Vpv*' ; (b) Space vector locations of voltage vector obtained from two-level inverter; (c) Schematic circuit diagram of dual-inverter fed OEWIM drive with input DC voltage (PV voltage) of

'*Vpv/2*'; (d) Space vector locations of voltage vector obtained from three-level dual-inverter scheme.

$$Vno = 1/3 (Vao +Vbo+Vco)= 1/3(SA+SB+SC)Vpv/2 \quad (17)$$

Thus, the space vector location of reference voltage vector OA(Fig. 4(b)) can be generated by the switching functions *SA*= 1, *SB*= -1 and *SC*= -1. Substituting these values in (17)

will result in the phase voltage, *van* as *2Vpv/3*. Now, consider the 3-phase, three-level dual-inverter connected to an OEWIM as shown in Fig. 4(c). Let the input PV source voltage is *Vpv/2,* which is half of the voltage taken for two-level H-bridge inverter. Now, the dual-inverter output phase voltage *OG* (Fig. 4(d)) is given as

$$Vaa, =Vao -Va,o, -Voo, \quad (18)$$

Where *Voo'* is the common mode voltage (Fig. 4(c)) which is given by

$$Voo, = 1/3 \; Vpv/4 \; [(SA-SA,)+(SB-SB,)+(SC-SC,) \quad (19)$$

$$Vao,=(2/3(SA-SA,) – 1/3[(SB-SB,)+(SC-SC,)])Vpv/4 \quad (20)$$

So, to generate voltage vector *OG* (Fig. 4(d)), the switching functions required are *SA*= 1, *SB*= -1 and *SC*= -1 ;*SA'* = -1, *SB'* = 1 and *SC'* = 1. Substituting these values in (20),

results in the phase voltage of magnitude *2Vpv/3* corresponding to phase *aa'*.Hence, to generate the phase voltage of *2Vpv/3* the PV source voltage required in case of two-level inverter is *Vpv* and in case of dual-inverter connected to OEWIM is *Vpv/2*. However, DSAZE PWM technique needs excess 15% of DC-link voltage to generate the rated motor phase voltage.

IV.CONTROL STRATEGY

The solar PV powered fed dual-inverter connected to OEWIM-pump drive is operated using a simple control strategy, which simultaneous accomplishes MPPT and DSAZE PWM integrated together. This integrated algorithm generates the required PWM control signals for the modular dual-inverter. The flowchart of control algorithm is shown in Fig. 5. The MPPT part of algorithm facilitates motor pump drive to extract maximum available power from the PV source, thereby assuring effective utilization of the PV

ISSN (Online) 2395-2717

International Journal of Engineering Research in Electrical and Electronic Engineering (IJEREEE)
Vol 2, Issue 8, August 2016

source. The DSAZE PWM part of the algorithm incorporates *V/f* control. It maintains constant rated flux in the motor which retains the maximum torque capability of the machine for the given PV power. Thus, in pump drive application where torque is proportional to square of speed, maintaining the maximum torque further helps in maximum utilization of the input source.

DSAZE PWM algorithm:

The magnitude of the reference voltage vector generated by the MPPT output and angle '*α*' is decomposed into the instantaneous three-phase reference voltage Vas, Vbs and Vcs for inverter-I. The gating time $Tgi(j=a, b, c)$ for top switches of inverter-I (Fig. 2) is then obtained by the switching algorithm. This algorithm requires instantaneous values of the reference phase voltage for calculating the effective time (time for which all the active vectors are switched) or turned ON time for top switches. The position of effective time period can be adjusted in such a way that the offset time is equal to Ts/2 within a switching period. This feature is exploited by DSAZE PWM technique to eliminate the zero sequence voltage within a sampling period. As DSAZE is a center spaced PWM technique for the Dual-inverter system, the ripple content in current is less and hence results in the improvement of developed torque.
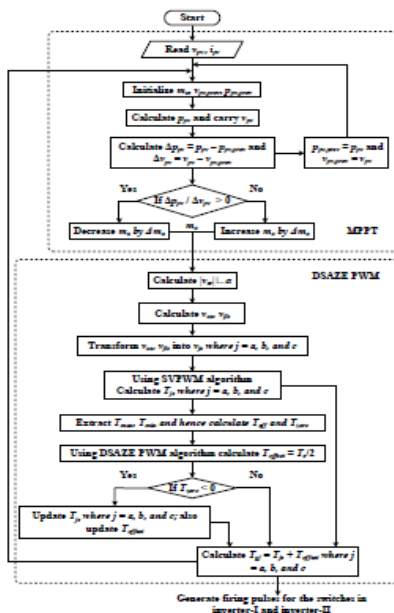
.
Fig. 5.Flow chart of the MPPT, DSAZE algorithm used in the proposed scheme

V. SIMULATION RESULTS WITH COST ANALYSIS

Simulation results:

The single-stage PV powered OEWIM drive for pump application, shown in Fig. 2 is simulated using MATLAB/Simulink. A 3.6 kW (20x3) PV array feeding power to a 4 kW OEWIM-pump drive is considered for simulation. The Solarex MSX60 PV panel parameters at Standard Test Conditions are Voc=21V,Isc=3.74A,Vm=17.1V,Im=3.5A,Pm=59.9W. A DC bus capacitor ($Cpvs$) of value 1000 μF is used at the output of PV source. A 4-pole,400V, 1430rpm induction motor is used. Further the important parameters of the motor are Rs=1.405□, Rr'=1.395□ xls=xlr'=1.8344□ xm=54.0982□. Simulations are performed by considering 96 samples per cycle of applied fundamental voltage, irrespective of the modulation index. This means that the switching frequency is a variable quantity. The switching frequency varies from 1.28 kHz (corresponding to a modulation index, ma = 0.2 with fundamental frequency f = 13.33Hz) to 4.8 kHz (corresponding to a modulation index, ma>= 0.75 with fundamental frequency f = 50Hz).

Fig. 6 shows the simulation results of the proposed system at different environmental conditions for PV source side parameters. The increasing and decreasing nature of PV power with respect to insolation (G) and temperature (T) can be observed with the waveforms of PV power and ma. This verifies the MPP tracking, further small oscillations in the value of ma near MPP and small ripple content in a PV power confirms the operation near optimum voltage. Also, another useful observation in the simulation results is that, the operating voltage of PV array passes through optimum voltage for every step increase in insolation and temperature. This can be justified with the matching values of peak power value during transient tracking and steady-state near MPP as given in the PV power subplot. Further, it can be noted that PV voltage waveform shows a sudden rise and fall in the value with the step increase in insolation and temperature. This can be attributed to charging and discharging of PV capacitor CPV with excess or deficit PV power respectively during transient condition.

Fig. 7 shows the motor side parameters for different environmental conditions. Variation on ma with respect to PV power can also be seen here in the waveform of torque, speed and mechanical power output. It can be

---

observed that torque, speed and mechanical power output follows *ma* or the PV power indirectly. Also, it can be easily observed that slip power too follows *ma*. Thus, slip power loss increases and decreases with increase and decrease of PV power respectively. This may help in keeping small variation in efficiency which can be observed from last subplot of Fig. 7. Also, another important feature that relate results of Fig. 6 and Fig. 7 is motor phase voltage plot. The transient variations in PV voltage *Vpv* during step increase in insolation can be depicted with a peak value of motor phase voltage waveform.

VI. CONCLUSION

In this paper, an integrated single-stage solution of PV fed pump drive is presented. The proposed system has the feature of low DC bus voltage requirement, MPPT integrated with *V/f*, presented. Implementation of *V/f* with MPPT can be verified with simulation and experimental results. Thus, a high performance integrated solution is proposed. Low cost of the proposed system can be attributed to the requirement of low voltage DC-link bus capacitor, low voltage rating switches and less.
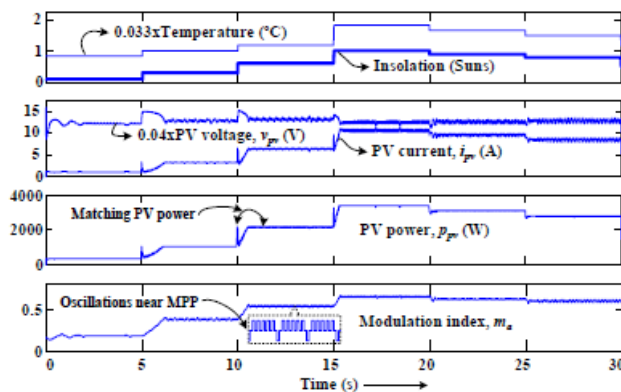
Fig. 6. Simulation results showing waveforms at PV source side.
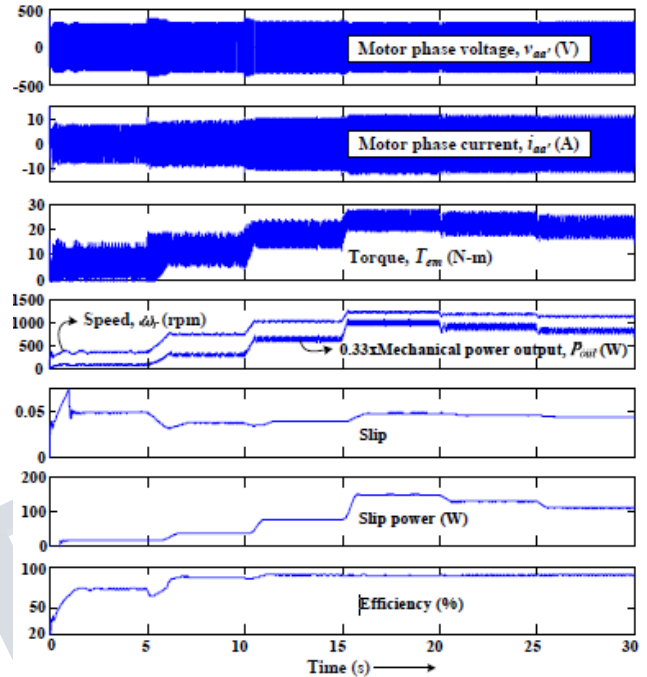
Fig. 7. Simulation results showing waveforms at motor-pump side

Number of sensors for the integrated control operation. Thus in all, this paper presents one of the effective and simple solutions for PV power fed water-pump application.

REFERENCES

[1] D. Maheswaran, K. K. Jembu Kailas, V. Rangaraj, W. AdithyaKumar,"Energy Efficiency in Electrical Systems", *Proc. of IEEE Inter. Conf. on Power Elect., Drives and Energy sys.,* pp 1-6, Dec. 2012.

[2] Y. Yao, P. Bustamante, R. S. Ramshaw, "Improvement of inductionmotor drive systems supplied by photovoltaic arrays with frequency control", *IEEE Trans. Energy Conv.*, vol. 9, no. 2, pp. 256-262, Jun.1994.

[3] Jogo Victor Mapurunga Caracas, Guilherme de CarvalhoFarias, LuisFelipe Moreira Teixeira, Luiz Antonio de Souza Ribeiro,"Implementation of a high-efficiency, high-lifetime and low-costconverter for an autonomous

photovoltaic water pumping system", *IEEETrans. Ind. App.,* vol. 50, no. 1, pp. 631-641, Jan./Feb. 2014.

[4] J. Appelbaum, "Starting and steady-state characteristics of dc-motorspowered by solar cell generators", *IEEE Trans. Energy Conv.*, vol. EC-1, no. 1, pp. 17-25, Mar. 1986.

[5] S. M. Alghuwainem, "Steady-state performance of DC motors suppliedfrom photovoltaic generators with step-up converter", *IEEE Trans.Energy Conv.*, vol. 7, no. 2, pp. 267-272, Jun. 1992.

[6] S. R. Bhat, Andre Pittet, B. S. Sonde, "Performance optimization ofinduction motor-pump system using photovoltaic energy source", *IEEE Trans. Ind. App.*, vol. IA-23, no. 6, pp. 995-1000, Nov./Dec. 1987.

[7] MontiêAlvesVitorino, MaurícioBeltrão de RossiterCorrêa, "An effective induction motor control for photovoltaic pumping", *IEEETrans. Ind. Elect.*, vol. 58, no. 4, pp. 1162-1170, Apr. 2011.

[8] Sachin Jain, VivekAgarwal, "A single-stage grid-connected invertertopology for solar PV systems with maximum power point tracking",*IEEE Trans. Power Elect.*, vol. 22, no. 5, pp. 1928-1940, Sep. 2007.

[9] Luiz Henrique S. Cabarets, Paulo PeixotoPrac¸a, Demercil S. OliveiraJr., and Ranoyca N. A. L. Silva "High-voltage gain boost converterbased on three-state commutation cell for battery charging using PV panels in a single conversion stage", *IEEE Trans. Power Elect.*, vol. 29, no. 1, pp. 150-158, Jan. 2014.

[10] Mario A. Herrán, Jonatan R. Fischer, Sergio Alejandro González, Marcos G. Judewicz and Daniel O. Carrica, "Adaptive dead-time compensation for grid-connected PWM inverters of single-stage PVsystems", *IEEE Trans. Power Elect.*, vol. 28, no. 6, pp. 2816-2825, Jun. 2013.